THE AMERICAN SOCIETY OF MECHANICAL ENGINEERS
345 E. 47th St., New York, N.Y. 10017

98-GT-542

THE EFFECT OF TURBULENCE ON THE HEAT TRANSFER IN CLOSED GAS-FILLED ROTATING ANNULI FOR DIFFERENT RAYLEIGH NUMBERS

Dieter Bohn and Jochen Gier
Institute of Steam and Gas Turbines
Aachen University of Technology
Germany

ABSTRACT

Higher turbine inlet temperatures are a common method of increasing the thermal efficiency of modern gas turbines. This development not only generates the need for more efficient turbine blade cooling but also demands a more profound knowledge of the mechanically and thermally stressed parts of the rotor. In order to determine thermal stresses from the temperature distribution in the rotor of a gas turbine, one has to encounter the convective heat transfer in rotor cavities. In the special case of a completely closed gas-filled rotating annulus the convective flow is governed by strong natural convection.

As shown in a previous paper by the authors, and for example by Owen, the presence of turbulence and its inclusion in the modeling of the flow has been found to cause significant differences in the flow development in rotating annuli. This influence in the special case of a closed rotating annulus has been recently investigated by the authors for a moderately high Rayleigh-Number. Based on this work an investigation was undertaken focusing on the development of turbulence and turbulence related changes in the flow structure for increasing Rayleigh-Numbers.

The flow is investigated numerically using a three-dimensional Navier-Stokes solver, based on a pressure correction scheme. To account for the turbulence, a low-Reynolds-number k-ε-model is employed. This model is complemented by an additional term for turbulence production due to buoyancy. The results are compared with experiments performed at the Institute of Steam and Gas Turbines. The computations demonstrate the considerable influence on the overall heat transfer as well as on the local heat transfer distribution.

NOMENCLATURE

a	thermal diffusivity ($a = \lambda/(\rho\, c_p)$)
a_c	centrifugal acceleration
b	distance between axial side walls
c	relative velocity in cavity
c_p	specific heat at constant pressure
H	distance between outer and inner cylindrical wall
L	length (here: height of cavity)
p	pressure
$\dot{q}$	heat flux from the hot to the cold wall
$\dot{q}_\lambda$	heat transfer by conduction alone
r	radius
R	gas constant
T	temperature
ΔT	temperature difference between hot and cold wall
(x,r,φ)	axial, radial, circumferential coordinate
v	velocity vector
h_t	total enthalpy
k	turbulent kintic energy
ε	turbulence dissipation
μ	dynamic viscosity
ρ	density
ω	angular velocity of the cavity
λ	thermal conductivity
α	section angle
C	constants

Subscripts:

i	inner
o	outer
m	arithmetical mean
max	maximum
min	minimum

$$Gr = \frac{r_m \cdot \omega^2 \cdot \Delta T \cdot L^3 \cdot \rho^2}{T_m \cdot \mu^2}$$ Grashof number

Presented at the International Gas Turbine & Aeroengine Congress & Exhibition
Stockholm, Sweden — June 2–June 5, 1998

$$Pr = \frac{\mu \cdot c_p}{\lambda} = \frac{\mu}{\rho \cdot a}$$ Prandtl number

$$Ra = Gr \cdot Pr$$ Rayleigh number

$$Re = \frac{\rho \cdot \omega \cdot r_m \cdot L}{\mu}$$ Reynolds number

$$Nu = \frac{\dot{q}}{\dot{q}_\lambda}$$ Nusselt number

INTRODUCTION

The development of gas turbines that operate at higher gas temperatures is a continuing trend to increase their thermal efficiency. This development requires careful design of the mechanically and thermally stressed parts. To estimate these stresses, a proper evaluation of temperature distributions in units and components operating in the hottest zones is necessary. In such a zone, temperature non-uniformities may lead to considerable additional stresses. Their acceptable value is also a function of the temperature level.

At present only an approximate estimation of the temperature distribution in a gas turbine rotor containing closed gas-filled enclosures (Fig. 1) is possible. In those cavities a strong, free convective flow is induced. This convection is caused by the buoyancy force corresponding to centrifugal acceleration and the different temperatures of the cavity walls. Such a flow increases the heat transfer throughout the cavities considerably.

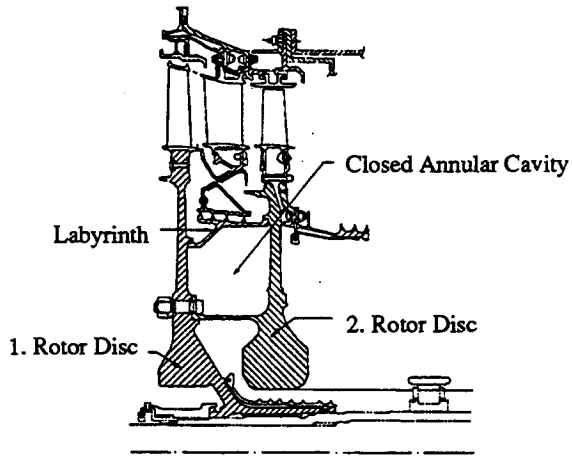

Figure 1: Rotating enclosure in a rotor

To date many theoretical and experimental investigations have been performed, to study the heat transfer in rotating enclosures with a throughflow of cooling fluid, e.g. Ong et al. (1991), Farthing et al. (1992), Owen et al. (1985). For sealed cavities with a purely free convection flow, the known theoretical and experimental investigations pertain mainly to constant temperature walls and are limited to qualitative descriptions of the convective processes. These investigations differ with respect to the direction of the heat flux in the cavity.

Most of the investigations were performed for an axially directed heat flux applied to a cylindrical rotating enclosure. For a rotating cavity with an entirely centripetal heat flux, Zysina-Molozhen and Salov (1977) experimentally analyzed the influence of rotational speed and various thermal boundary conditions on the heat transfer in a rotating annular enclosure. Using photographs, they noted the absence of any regular fluid circulation contours in the cavity. Lin and Preckshot (1979) calculated the temperature, velocity and streamline distribution for relatively low rates of acceleration.

Experimental and theoretical investigations of the heat transfer in a closed rotating cavity with a centripetally directed heat flux were carried out in a previous paper by Bohn et al. (1995). There, the feasibility of numerical prediction for the flow and heat transfer was shown and some flow instabilities were found. However, these computations were conducted only with the assumption of laminar flow inside the cavity.

There are a number of publications on the numerical simulation of turbulent flows in cavity configurations with throughflow and rotor-stator systems. For turbulence modeling most authors use variations of low-Reynolds k-ε models, e.g. Gan et al. (1996) and Iacovides et al. (1996). There are other approaches, too, such as Reynolds-Stress modeling, e.g. Iacovides et al. (1996) and Izenson et al. (1995), and multiple scale k-ε models (Guo and Rhode, 1995).

In a previous paper (Bohn and Gier, 1997) using a low Re-number k-ε model the authors have shown as a first step that for a moderate Ra-number the heat transfer intensifying effect of turbulence is larger than the damping effect of turbulence-induced higher shear. However, it is important to investigate this influence in more detail and see its development as the Ra-number increases closer to typical values found in state-of-the-art gas turbines.

To assess this influence, in this paper the same closed rotating annulus with a 45° segmentation as employed in the previous paper (Bohn & Gier, 1997) is used for the numerical study (Fig. 2). Results are analyzed for 3 different Ra-numbers .

The segmented annulus is chosen because it requires considerably less computational effort and exhibits a much more stable flow structure than an open annulus, which is important for analyzing the basic effects.

By analyzing the basic conservation equations of mass, momentum and energy (see below) it can be demonstrated that

$$Nu = f(Ra, Re, Pr, H/r_m, b/r_m) \quad (1)$$

The Nusselt number (Nu) is defined as the ratio of the heat flux throughout the cavity to that flux which would occur in solid-body rotation without any motion relative to a co-rotating frame of reference. Thus, Nu is equal to unity for no convection and is greater than unity when convection takes place. The rotational Rayleigh number (Ra) is the product of the Grashof number and the Prandtl number and is related to the buoyancy term in the radial momentum equation. The rotational Reynolds number (Re) has its origin in the Coriolis force terms in the momentum equations. In contrast to the case of an axially directed heat flux its influence is relatively small for the centripetal heat flux (Bohn et al., 1996). Because of this, all

chosen points of operation can be expected to be in the turbulent flow regime ($Ra > 10^9$).

NUMERICAL PROCEDURE

The flow in the rotating cavity is described by the Navier-Stokes conservation equations for mass (2), momentum (3) and energy (4). In common tensor form, these equations read:

$$\nabla\cdot(\rho\vec{v}) = 0 \tag{2}$$

$$\nabla\cdot(\rho\vec{v}\otimes\vec{v}) - \nabla\cdot(\mu_{eff}\nabla\vec{v}) = -\nabla\left(p+\frac{2}{3}k\right) + \nabla\left(\mu_{eff}(\nabla\vec{v})^T\right) \tag{3}$$

$$\nabla\cdot(\rho\vec{v}h_t) - \nabla\cdot\left(\frac{\lambda}{c_p}+\frac{\mu_t}{Pr_t}\right)\nabla h_t = 0 \tag{4}$$

Some important assumptions should be mentioned in this regard. The equations (2) - (4) are valid for a compressible, steady-state flow. In case of turbulent flow all primitive variables are density-weighted averaged (Favre). A cylindrical coordinate system (z,r,φ) has been used, in which r=0 identifies the axis. In this system the Nabla-operator becomes:

$$\nabla = \partial/\partial z + \partial/\partial r + 1/r\,\partial/\partial\varphi$$

The computations of the rotating cavity are carried out within a rotating frame of reference. This results in additional centrifugal and Coriolis force terms in the momentum equations and the energy equation. The set of equations is closed by the ideal gas law.

Turbulence effects

The eddy viscosity hypothesis has been used to take turbulence effects into account, hence the effective viscosity μ_{eff} is the sum of the laminar viscosity μ and the turbulent viscosity μ_t. Two additional equations for the turbulent energy k (5) and the dissipation rate ε (6) have to be solved in order to calculate the turbulent viscosity which is not a fluid property but which depends on the flow field. The low-Reynolds-version of Launder and Sharma (1974) has been used (5, 6 and 7):

$$\nabla\cdot(\rho\vec{v}k) - \nabla\cdot\left(\left(\mu+\frac{\mu_t}{Pr_t}\right)\nabla k\right) = \mu_t\nabla\vec{v}\cdot\left(\nabla\vec{v}+(\nabla\vec{v})^T\right) - \frac{2}{3}\nabla\cdot\vec{v}(\mu_t\nabla\cdot\vec{v}+\rho k) - \rho\varepsilon - 2\mu\left(\nabla k^{\frac{1}{2}}\right)^2 \tag{5}$$

$$\nabla\cdot(\rho\vec{v}\varepsilon) - \nabla\cdot\left(\left(\mu+\frac{\mu_t}{Pr_{t,\varepsilon}}\right)\nabla\varepsilon\right) = C_1\frac{\varepsilon}{k}\cdot\left(\mu_t\nabla\vec{v}\cdot\left(\nabla\vec{v}+(\nabla\vec{v})^T\right) - \frac{2}{3}\nabla\cdot\vec{v}(\mu_t\nabla\cdot\vec{v}+\rho k)\right) - C_2 f_2\rho\frac{\varepsilon^2}{k} + 2\frac{\mu\mu_t}{\rho}(\nabla\nabla\vec{v})^2 \tag{6}$$

$$\mu_t = C_\mu f_\mu \rho\frac{k^2}{\varepsilon} \tag{7}$$

The model involves a damping of the effective viscosity (7) when the local turbulent Re number is low. Also the source terms of the k and ε equation are modified. The empirical functions f_μ and f_2 are defined by:

$$f_\mu = \exp\left(\frac{-3.4}{(1+0.02\,Re_t)^2}\right) \tag{8}$$

$$f_2 = 1 - 0.3\exp\left(-Re_t^2\right) \tag{9}$$

where the local turbulent Reynolds number is given by:

$$Re_t = \frac{\rho k^2}{\mu\varepsilon} \tag{10}$$

The Launder-Sharma model is used because it allows the calculation of μ_t without any explicit dependence of the model functions on the wall distance. This is an important feature for a closed configuration like the rotating cavity. The model is widely used for transitional as well as fully turbulent flows.

For some calculations the flow-destabilizing and thus turbulence-increasing effect of buoyancy has been modeled through inclusion of an additional source term in the k- and ε-equations,

$$G = -\frac{\mu_{eff}}{\rho\sigma_T}\vec{a}_c\cdot\nabla\rho \tag{11}$$

with a_c as the centrifugal acceleration. The constants in the model are given in Table 1.

$Pr_{t,h}$	$Pr_{t,k}$	$Pr_{t,\varepsilon}$	C_1	C_2	C_μ	C_3	σ_T
0.9	1	1.217	1.44	1.92	0.09	1	0.9

Table 1: Constants of the employed turbulence model

Numerical scheme

A modern fully implicit Finite-Volume-scheme has been used for solving the set of partial differential equations (2-6) numerically. The SIMPLEC pressure-correction (Van Doormal and Raithby 1984) algorithm is adapted on a non-staggered grid, while avoiding the chequerboard oscillations by using the improved Rhie-Chow interpolation method (Rhie and Chow 1983). For the diffusion terms a central differencing scheme is used, while the advection terms are discretised by hybrid differencing, in which central differencing is used if the mesh Peclet number is less than 2, and upwind differencing if the mesh Peclet number is greater than 2.

Boundaries and mesh

In Figure 2 the calculated cavity is shown schematically. The computational domain and boundary conditions are

equivalent to an experimental setup reported by Bohn et al. (1995, 1996).

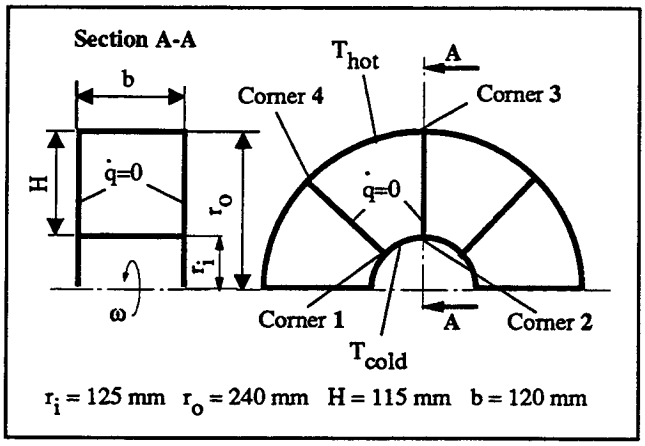

Figure 2: Dimensions of the annular cavitiy

The domain consists of an annulus segmented into eight 45°-segments. These are separated from each other by insulating walls. The outer radius is heated up to a constant temperature and the hub is cooled down to a constant temperature. All other walls are assumed to be adiabatic. At the walls the velocity (within the frame of reference) is zero. Three cases with different Ra-numbers are computed (Table 2).

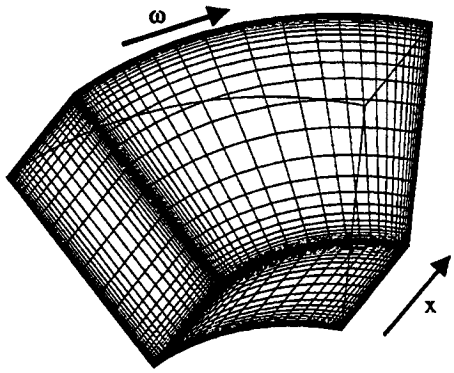

Figure 3: Three-dimensional computational grid

For case C1 and C2 the computational mesh has been refined once resulting in only slight differences in the solution. The results in this paper are all taken from the finer mesh, consisting of 38 cells in radial, 30 cells in axial and 34 cells in circumferential direction with a total of 38760 cells, which is approximately 2 times more than the coarser mesh. It is shown in Fig. 3. Case C3 is calculated with a finer mesh consisting of 83160 cells, which is necessary due to the higher Ra-number. The meshes are refined in the boundary layer region giving a y^+_{max} at the heated and cooled wall of 0.6 and on the other walls of 1.4.

RESULTS

In order to assess the influence of a variation of the free convection driving force characterized by the Ra-number, three different Ra-number conditions are compared. The lower Ra-number of $1.638 \cdot 10^9$ is the same as reported by Bohn and Gier (1997). All computations were converged several orders of magnitude ensuring steady state conditions. The difference between the integral heat flux into the cavity and out of the cavity was small (<6 %, approaching steady state asymptotically) and the flow variables at several characteristic locations had approached constant values.

The basic flow structure in the sectored cavity is very similar for the two Ra-numbers shown in Fig. 4. In the case of a laminar flow assumption, cases C1 and C3 both look very similar. Corner vortices exist in all corners. There is also some fluid motion in the center of the cavity in both cases. Note however that the velocity magnitude (c_{max}) is about 3 times larger for the higher Ra-number (Table 2).

case	C1 (lam/turb)	C2 (lam/turb)	C3 (lam/turb)
Ra-#	$1.638 \cdot 10^9$	$9.985 \cdot 10^9$	$2.437 \cdot 10^{10}$
Re-#	$2.151 \cdot 10^5$	$5.955 \cdot 10^5$	$9.599 \cdot 10^5$
ΔT	26.1 K	20.8 K	19.9 K
c_{max}	1.09 / 0.89 m/s	2.25 / 1.784 m/s	3.46 / 2.75 m/s
k_{max}	0.05 m^2/s^2	0.20 m^2/s^2	0.35 m^2/s^2

Table 2: Selected boundary conditions and results of investigated cases

The presence of turbulence causes higher effective shear stresses within the flow. These stresses not only damp the weak vortices in the cavity center, resulting in a vanishing fluid motion according to the Taylor-Proudman Theorem, but they also affect the shape of the corner vortices.

It is interesting to note that in the higher Ra-number case (C3) the vortices in corners 2 and 4 (Fig. 2) basically vanish, which does not happen in case C1. The reason can be seen in increased turbulent viscosity. The fact that corner vortices 1 and 3 are not significantly reduced in size proves, as already discussed by Bohn & Gier (1997), that these vortices are additionally driven by buoyancy forces, which are increased due to the turbulence induced strenghth of the heat flux at the cylindrical walls. The convex and concave shape, respectively, of the cylindrical walls is responsible for the different size and shape of the corner vortices, as described in the previous paper of Bohn & Gier (1997).

Increasing the Ra-number, which characterizes the driving forces for the fluid motion inside the closed cavity, leads to increased velocities and turbulent kinetic energy (Table 2 and Fig. 5). In cases C1 and C3, the impingement regions in corners 1 and 3 exhibit the highest levels of turbulence, especially near the inner cylindrical wall. Here, turbulence is produced due to a strong flow deceleration. This deceleration leads to a flow

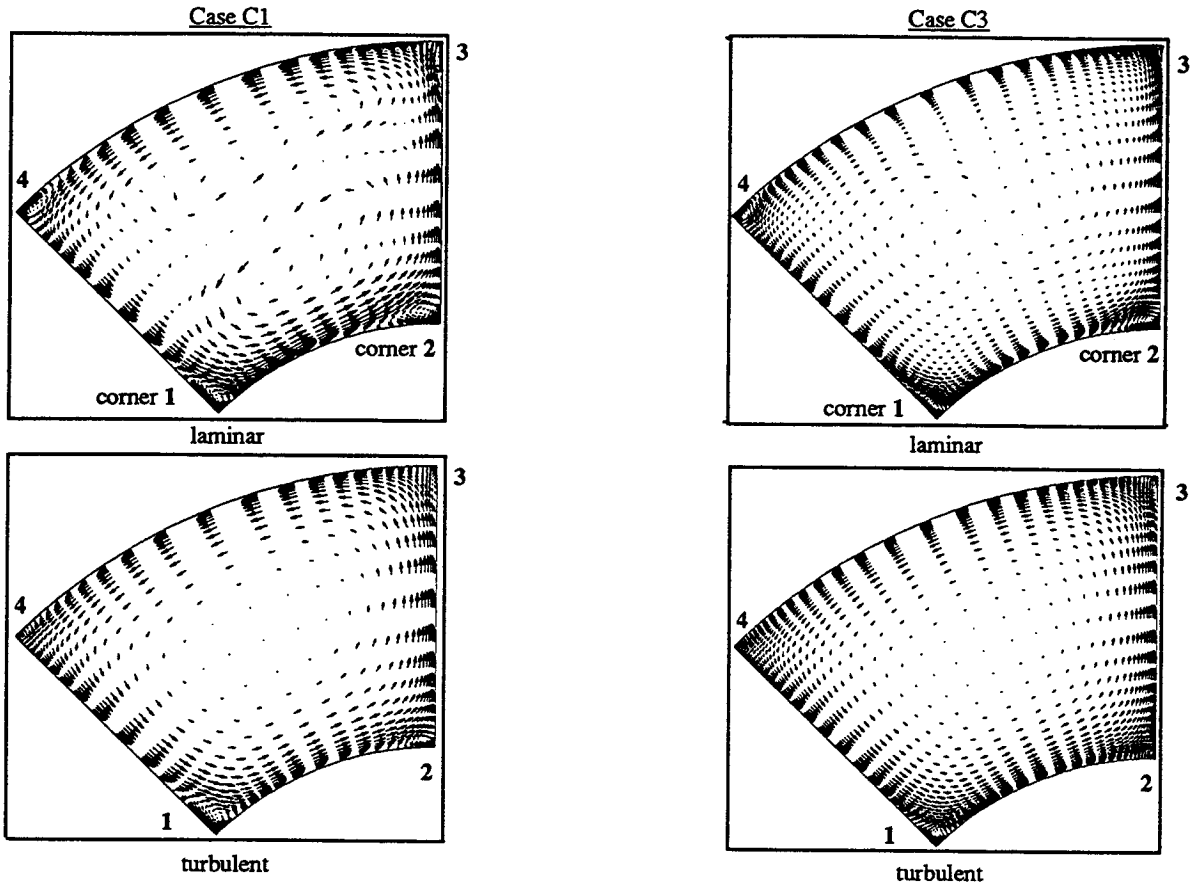

Figure 4: Velocity vectors in the cavity (middle section: x/b = 0.5, vector scale different for cases C1 and C3)

destabilization, which enhances turbulence production. This effect is stronger, the stronger the deceleration, and thus the turbulence maximum is located close to corner 1. Downstream of this impingement region, where the flow is accelerated again, turbulence is damped. Here, the shear in the flow is not sufficient to produce enough turbulence to maintain the turbulence level. Although the level of the turbulence energy is of course different in cases C1 and C3, the turbulence degree, defined $Tu = (\sqrt{k})/c_{max}$ is quite similar as are the main features of the distribution.

As already seen, increasing the Ra-number leads to a stronger convective flow motion. This further increases the ratio of heat transported by convection to heat transported by diffusion (conduction). This becomes obvious from Figure 6. The thermal boundary layers are thinner in case C3 and the basically isothermal core region is larger.

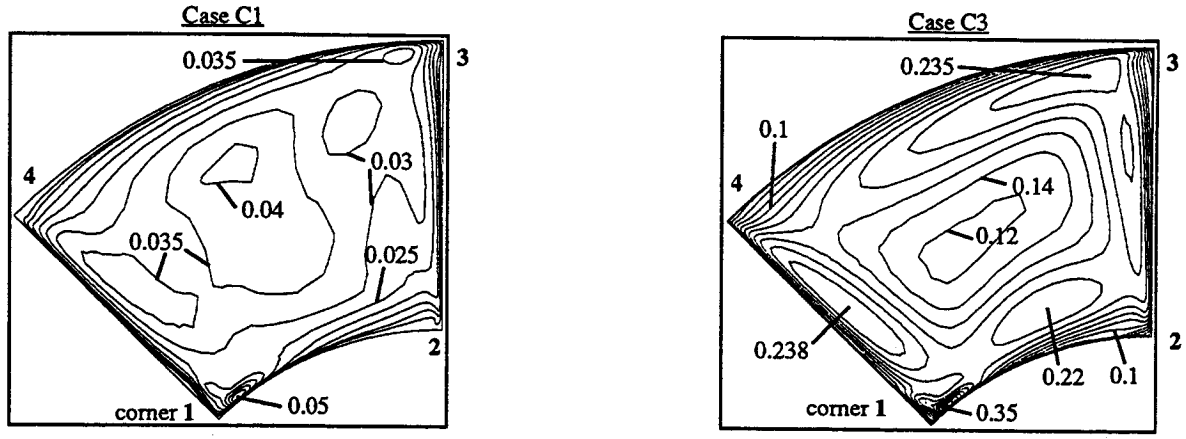

Figure 5: Isolines of turbulent energy k [m^2/s^2] in the cavity (middle section: x/b = 0.5)

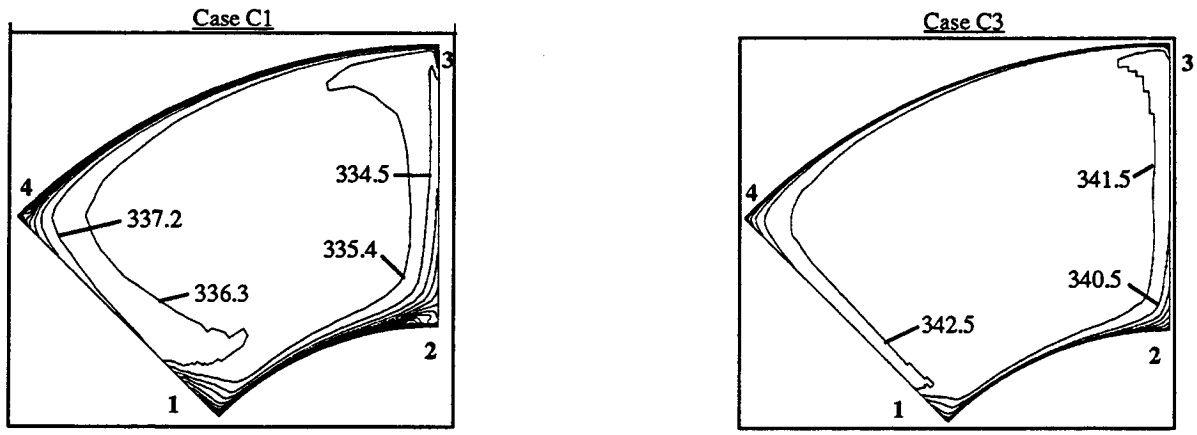

Figure 6: Isolines of temperature [K] in the cavity (middle section: x/b = 0.5)

Thus a larger Ra-number leads to an increased convective fluid motion, which then causes increased turbulence and heat transfer, leading to a further enhanced flow. And, as already shown by the authors in the previous paper (1997), the heat flux intensifying effect of turbulence is larger than the convective heat transfer damping effect of the turbulence-induced higher shear.

The differences in the convective flow motion have a significant impact on the local heat flux distribution on the cylindrical walls. Because the velocities are larger in the case of the larger Ra-number, the heat transfer on the walls is intensified. However, the local heat flux is only approximately twice as large in case C3 as in case C1 in most parts of the wall, but it is 4 times larger in the impingement region (Fig. 7 & 8). The perception is that increasing the Ra-number for the closed, rotating cavity not only leads to enhanced integral heat transfer, but also results in a significantly increased ratio of the maximum and minimum local heat flux on the cylindrical walls.

Although linear k-ε models generally tend to somewhat overpredict the heat flux in impimgement zones, the heat flux level prediction with the current model is still sufficiently reliable. The effect described above, which takes place on both cylindrical walls, will cause larger temperature differences in the rotor material in real machines as the Ra-number increases.

This locally high heat flux in the impingement region also explains why the corner vortices 1 and 3 are not reduced in size by the presence of turbulence. Turbulence further increases the local heat flux in the impingement region. For example, in corner 1 the fluid is cooled down in the impingement zone and its density is thus increased. This causes buoyant forces to enhance the vortex motion. Turbulence introduces additional shear, but due to the much intensified heat transfer in the impingement regions the local heat flux in corners 2 and 4 is reduced because the fluid already exchanged much heat at impingement. The buoyancy forces, additionally driving corner vortices 1 and 3, are too weak to substantially enhance vortex motion in corners 2 and 4. This damps these vortices in case C1 and they vanish entirely in case C3. Hence, this is a strong indicator that the influence of turbulence grows as the Ra-number increases.

The largest local heat flux gradients occur on the cylindrical walls in circumferential direction. But especially on the outer cylindrical wall, the flow structure changes with Ra-number in some respect. In addition to the circumferential inhomogeneities

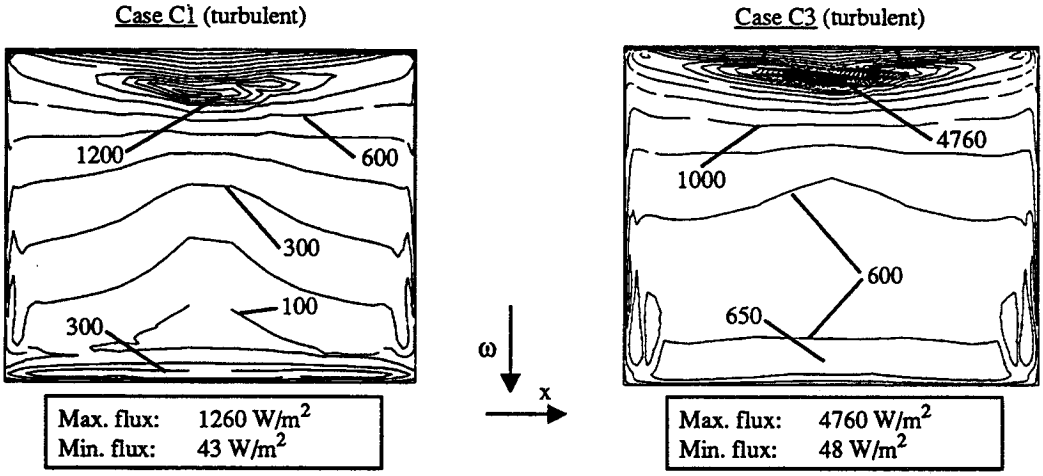

Figure 7: Isolines of heat flux through inner cyl. wall (cold wall)

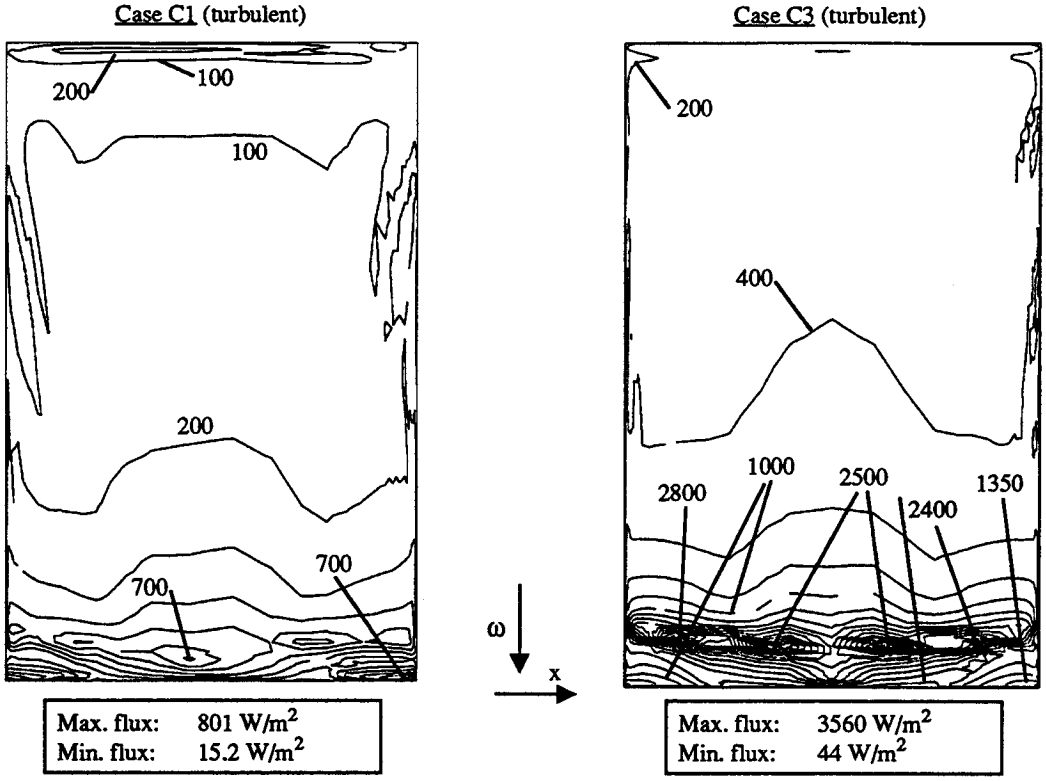

Figure 8: Isolines of heat flux through outer cyl. wall (hot wall)

there are also local maxima in axial direction in the impingement region. While in case C1 there is one maximum in the mid-axial position and two relative maxima near the axial side walls, there are 4 local maxima along one axial line in case C3 (Fig.8).

These distributions hint strongly at 3-dimensional effects in the cavity flow. As reported in the previous paper by the authors (1997), the 3-dimensional effects have a significant impact on the local heat flux, although the integral flow properties are hardly affected. These 3-dimensional effects become even more significant for higher Ra-numbers, as can be seen through comparison of C1 and C3 in Figure 8. In case C3 the local heat flux intensity varies between 1600 W/m^2 and 3500 W/m^2 along an axial line in the impingement region, which is a factor of 2.

The mechanism can be analysed with help of Figure 9. There one can see several streamlines in one part of the cavity cut out of the entire domain for post-processing, which includes corners 2 and 3.

While streamlines Sl 1 and Sl 3 make a 90° turn in corner 3, streamlines Sl 2 and Sl 4 move through the corner vortices towards the axial side walls. Hence, the flow in the axial center of the cavity splits up into a branch performing just a 90° turn and afterwards flowing along the outer cylindrical wall and two branches filling up the corner vortex and eventually leaving it near the axial side walls. The flow adjacent to the axial mid position is somewhat faster and impinges more strongly than in midspan position itself, leading to the maximum heat flux intensity.

This is different for the lower Ra-case C1, where the maximum heat flux is located near the middle position. In the corners between the cylindrical wall, the axial and circumferential sector separation walls the corner vortex weakens and the flow directed radially outwards moves along the sector separation wall and forms a vortex, counter-rotating with respect to the corner vortex. This can be seen through streamline 4 and vector plot for x/b=0.98 in Figure 9.

Near to the axial side wall, the convective flow motion is damped. This leads to a weaker local heat flux at the impingement point, resulting in weaker buoyancy forces. And these, as already mentioned, are necessary to maintain a strong corner vortex despite turbulence-induced high shear. This mechanism is responsible for the local heat flux maximum in the corner of the axial side wall and the segmentation wall.

Generally speaking, the strong interaction between flow and heat transfer in this closed cavity, where the flow motion is only caused by buoyancy, which itself is strongly dependent on the flow, is the reason for this complex flow structure. The degree of complexity increases with growing Ra-number.

In order to include the stabilizing / destabilizing effect of buoyancy on the turbulent flow resulting in a decrease / increase of turbulence production, one can add additional source terms to the k and ε equation. Such a source term has been included in the code in order to assess its influence on the heat transfer and flow inside this closed rotating cavity.

Turbulence generation due to shear and due to buoyancy is

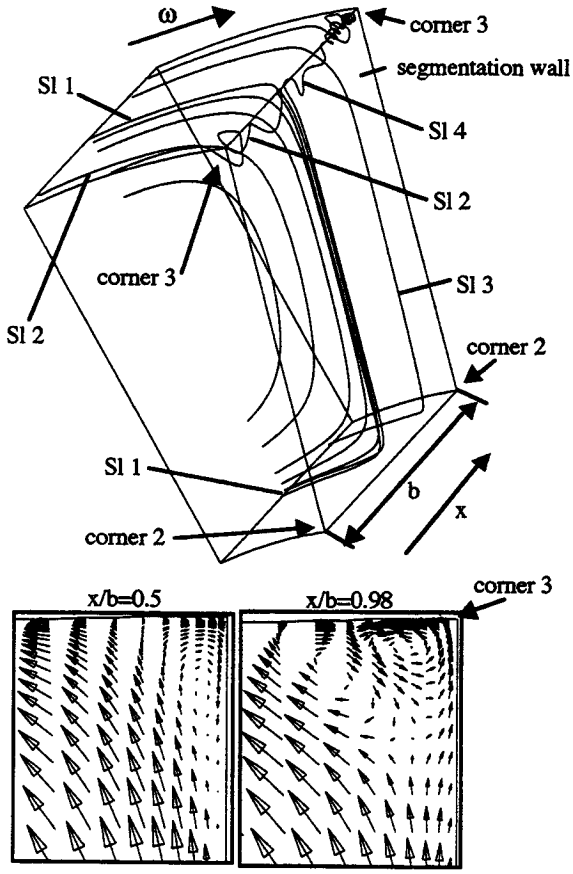

Figure 9: Streamlines in region of corners 2 & 3 and vectors in middle and near axial wall section cut, case C3, turb.

dependent on the Ra-number in a different way. While the production due to buoyancy is directly dependent on the Ra-number through the density gradients and the acceleration field, the production due to shear is indirectly dependent on the Ra-number through the convective flow motion.

The integral Nu-numbers obtained for the computations are shown in Figure 10.

Laminar and turbulent computation (without additional source terms) of case C1 exhibit only a relatively small difference in terms of the Nu-number, while for the two other cases the turbulent flow causes a 50 % increase in the Nu-number. Including buoyancy sources for turbulence has a relatively small impact on the integral heat transfer for the setup investigated in this paper, although this effect is stronger for the lower Ra-number cases. The reason is that the buoyancy source term can either damp or enhance turbulence production, depending on the local direction of the density gradients. Hence, this models the stabilizing / destabilizing effect of these gradients on the flow. In the rotating cavity with centripetal heat flux the density gradient and the centrifugal acceleration are of opposite direction in the boundary layers at the cylindrical walls, enhancing turbulence production. However, as can be seen from Figures 6 and 7, most of the heat is transfered in the impingement regions, where turbulence production due to shear

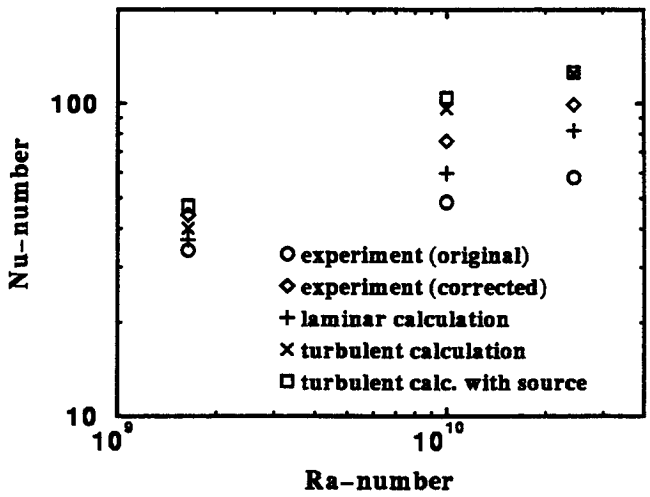

Figure 10: Mean Nusselt-number for investigated cases C1 - C3

is much larger. Thus the additional production only has relatively little impact through increasing the turbulence degree in the cavity regions with little flow motion. Hence, this turbulence increases the heat transfer in the cavity core and acts like an intensified heat conduction This impact is larger in the low Ra-number case C1, because there the convective heat transfer, driven by the flow motion, is smaller than in the high Ra-number cases.

Also experimental results based on measurements of Gorzelitz (1994) are included in Figure 10. There, the original value and the corrected value are given for each Ra-number. The original value does not take into account the heat flux through the axial side walls, which is between 20 % and 30 % of the total heat flux into the cavity. This heat flux cooles down the hot air flowing radially inwards and is thus damping the convective flow motion. This effect is equivalent to a reduction of the global Ra-number, which charcterizes the forcing of the convective flow motion. Since the side walls are computed as ideally adiabatic, a correction of the mean Nu-number is given in equation 12:

$$Nu_{corr} = Nu\,(Ra_{corr})$$

$$Ra_{corr} = s \cdot Ra_{orig}^{\ t} \quad \text{with: } s = 1/1500,\ t = 1.406 \qquad (12)$$

The coefficient t is determined by evaluating the effect of the loss heat flux based on the flow structure. The factor s is then determined by fixing this function to the Ra_{corr} value in Case C1. Additional uncertainties occur with respect to the general measureing tolerances, heat conductivity of the heat flux measuring layer and not perfectly isothermal inner cylindrical wall.

This experimental data supports the general development of the Nu-number as a function of the Ra-number. Due to the tolerance of the experimental values they can neither prove nor disprove the location of the transition range between Ra-numbers of 10^9 to 10^{10}. However, it is well known, that for many buoyancy induced flows transition to turbulent flow

occurs at Ra-numbers of about 10^9. While this limit is higher, if the Coriolis forces have a strongly damping effect on the buoyancy driven flow like in the case of an axial heat flux inside the cavity (Owen, 1995), they do not damp the flow in the radial flux case investigated in this paper (Bohn et al, 1996).

SUMMARY AND CONCLUSIONS

Investigations have been carried out on the convective heat transfer in a closed rotating annulus with 45° segmentation and with a purely radial heat flux imposed. While the inner and outer cylindrical walls were held at a constant temperature, the side walls were thermally insulated.

The influence of the Ra-number on the turbulence and thereby on the heat flux through the cavity was investigated through comparison of computations for 3 different Ra-numbers.

By comparing computations for the different Ra-numbers it was discovered that the influence of turbulence becomes stronger for larger Ra-numbers. Also, not only do the integral Nu-numbers increase with growing Ra-numbers but the differences in the local heat flux distribution on the cylindrical walls increase twice as much. This is partly due to the increasing intensity of 3-dimensional effects and the growing complexity of the flow for larger Ra-numbers. The impact of turbulence enhances this even more.

Including an additional source term to account for buoyancy-induced turbulence production was found to have only little influence on the development of the flow for the case investigated.

Because modern high temperature gas turbines operate under conditions with even somewhat larger Ra-numbers, the increase in temperature differences caused by the growing heat flux inhomogeneities should be considered in the design process.

The convective heat transfer for this type of flow can be computed with laminar flow assumption already quite well. If turbulence occurs, which could not be definitely determined through experimental data, it can also be simulated with the employed appraoch. The authors hope, that with a new test rig currently under construction , it will be possible to gather more reliable experimental data for these high Ra-numbers.

Further investigations should extend these results to other points of operation with even larger Ra-numbers as well as to the unsectored rotating annulus, in which additional aspects of the flow stability occur.

ACKNOWLEDGEMENTS

This work was funded by the German Research Foundation DFG (Deutsche Forschungsgemeinschaft). The authors greatfully acknowledge the German Reasearch Foundation for the permission for publication.

REFERENCES

Bohn, D., Deuker,E., Emunds, R., Gorzelitz, V., 1995, "Experimental and Theoretical Investigations of Heat Transfer in Closed Gas-Filled Rotating Annuli", *J. of Turbomachinery*, Transactions of the ASME, Vol. 117, No. 1, pp. 175 - 183

Bohn, D., Emunds, R., Gorzelitz, V., Krüger, U., 1996, "Experimental and Theoretical Investigations of Heat Transfer in Closed Gas-Filled Rotating Annuli II", *J. of Turbomachinery*, Transactions of the ASME, Vol. 118, No. 1, pp. 11 - 19

Bohn, D., Gier, J., 1997, "The Effect of Turbulence on the Heat Transfer in Closed Gas-Filled Rotating Annuli", ASME Paper 97-GT-242, to be published in Transactions of the ASME

Farthing, P.R., Long, C.A., Owen, J.M., Pincombe, J.R., 1992, "Rotating Cavity with Axial Throughflow of Cooling Air: Heat Transfer", *ASME Journal of Turbomachinery*, Vol. 114, pp. 229-236

Gan, X., Mirzaee, I., Owen, J.M., Rees, D.A.S., Wilson, M., 1996, "Flow in a Rotating Cavity with a Peripheral Inlet and Outlet of Cooling Air", ASME Paper 96-GT-309

Gorzelitz, V., 1994, "Experimentelle Untersuchung des Wärmetransportes in geschlossenen kreisringförmigen rotierenden Hohlräumen", PhD-thesis, Aachen University of Technology

Guo, Z., Rhode, D.L., 1995, "Assessment of Two- and Three-Scale k-ε Models for Rotating Cavity Flows", ASME Paper 95-GT-300

Iacovides, H., Nikas, K.S., Te Braak, M.A.F., 1996, "Turbulent Flow Computations in Rotating Cavities using Low-Reynolds-Number Models", ASME Paper 96-GT-159

Izenson, M., Kennedy, M.R., Sirukudi, J.R., 1995, "Turbulent Flow Computations for Turbine Disc Cavity Flows", ASME Paper 95-GT-192

Launder, B.E., Sharma, B.T., 1974, "Application of the Energy Dissipation Model of Turbulence to the Calculation of Flow near a Spinning Disc", *Lett. Heat and Mass Transfer 1*, pp. 131-138

Lin, T.Y., Preckshot, G.W., 1979, "Steady State Laminar Natural Convection in a Rotating Annulus", *Studies in Heat Transfer, A Festschrift for E.R.G. Eckert*, Hemesphere Publishing Corporation, pp. 219-246

Ong, C.L., Owen, J.M., 1991, "Prediction of Heat Transfer in a Rotating Cavity with a Radial Outflow", *ASME Journal of Turbomachinery*, Vol. 113, pp. 115-122

Owen, J.M., Pincombe, J.R., Rogers, R.H., 1985, "Source-Sink Flow Inside a Rotating Cylindrical Cavity", *J. Fluid Mech.*, Vol. 155, pp. 233-265

Owen, J.M., Rogers, R.H., 1995, "Flow and Heat Transfer in Rotating-Disc Systems", Vol. 2 Rotating Cavities, Wiley & Sons

Rhie, C.M., Chow, W.L., 1983, "Numerical Study of the Turbulent Flow past an Airfoil with Trailing Edge Separation. ", *AIAA Journal*, Vol. 21, pp. 1527-1532

Van Doormal, J.P., Raithby, G.D., 1984, "Enhancements of the SIMPLE Method for Predicting Incompressible Fluid Flows", *Num. Heat Transfer*, Vol. 7, pp. 147-163

Zysina-Molozhen, I.M., Salov, N.N., 1977, "Heat Exchange and Flow Regime of Liqiuds in a Closed Ratating Annular Cavity", *Soviet-Aeronautics*, Vol. 20, No. 1, pp. 39-43